JTTEE5 17:329–337
DOI: 10.1007/s11666-008-9181-5
1059-9630/$19.00 © ASM International

Deposition of Al_2O_3-TiO_2 Nanostructured Powders by Atmospheric Plasma Spraying

E. Sánchez, E. Bannier, V. Cantavella, M.D. Salvador, E. Klyatskina, J. Morgiel, J. Grzonka, and A.R. Boccaccini

(Submitted September 7, 2007; in revised form April 9, 2008)

Al_2O_3-13%TiO_2 coatings were deposited on stainless steel substrates from conventional and nanostructured powders using atmospheric plasma spraying (APS). A complete characterization of the feedstock confirmed its nanostructured nature. Coating microstructures and phase compositions were characterized using SEM, TEM, and XRD techniques. The microstructure comprised two clearly differentiated regions. One region, completely fused, consisted mainly of nanometer-sized grains of γ-Al_2O_3 with dissolved Ti^{+4}. The other region, partly fused, retained the microstructure of the starting powder and was principally made up of submicrometer-sized grains of α-Al_2O_3, as confirmed by TEM. Coating microhardness as well as tribological behavior were determined. Vickers microhardness values of conventional coatings were in average slightly lower than the values for nanostructured coating. The wear resistance of conventional coatings was shown to be lower than that of nanostructured coatings as a consequence of Ti segregation. A correlation between the final properties, the coating microstructure, and the feedstock characteristics is given.

Keywords Al_2O_3-TiO_2, nanostructured coatings, thermal spraying

1. Introduction

Nanostructured materials represent an enhanced version of their conventional counterparts (Ref 1, 2) and usually exhibiting better performances (Ref 3-5). Bulk nanomaterials are being extensively studied but also nanostructured coatings on conventional materials are investigated as they have the potential of providing several industries with novel materials with improved properties and prolonged lifetime (Ref 6-8).

Thermal spray techniques such as plasma spraying, in which a powder is injected into plasma, molten, and accelerated toward a substrate where it impacts creating a coating, are widely used in industry (Ref 9). The production of nanostructured coatings using such conventional techniques would be especially interesting if only changes of the raw material would be required, as no expensive investment would be necessary. Unfortunately, nanoparticles cannot be sprayed because of their low mass and poor flowability. However, several studies have shown that this problem can be solved by agglomerating them in micrometer-sized aggregates, which can be sprayed as easily as conventional powders (Ref 10-13). Commercial agglomerated nanopowders are now available. However, the process must be carefully controlled in order to keep the initial nanostructure in the final coating (Ref 14-16). Typical nanostructured ceramic coatings obtained by plasma spraying from agglomerated powders include alumina (Ref 17), alumina-titania (Ref 18, 19), cemented tungsten carbides (Ref 20, 21), or zirconia (Ref 22, 23).

In this work, alumina-titania ceramic coatings were obtained by atmospheric plasma spraying (APS) using commercial micrometric and nanostructured powders. Both feedstock were completely characterized before deposition. Then, the microstructure of the newly developed nanostructured coatings was studied, relevant properties were measured and, where appropriate, comparison with equivalent conventional coatings (e.g., obtained from micron-sized powders) is presented.

2. Experimental Techniques

2.1 Materials

Oxide (Al_2O_3-13wt.% TiO_2) coatings were obtained from commercial feeding-powders (one conventional from Sulzer Metco, Germany, and the other nanostructured from Inframat Advanced Materials, USA). Both materials' characteristics are given in Table 1, which indicates that the nanostructured feedstock also contains zirconium oxide and cerium oxide. Such additives are mainly added

E. Sánchez, E. Bannier, and **V. Cantavella**, Instituto de Tecnología Cerámica, Asociación de Investigación de las Industrias Cerámicas, Universitat Jaume I., Castellon, Spain; **M.D. Salvador** and **E. Klyatskina**, Instituto de Tecnología de Materiales, Universidad Politécnica de Valencia, Valencia, Spain; **J. Morgiel** and **J. Grzonka**, Institute of Metallurgy and Materials Science, Krakow, Poland; and **A.R. Boccaccini**, Department of Materials, Imperial College London, London SW7 2BP, UK. Contact e-mail: emilie.bannier@itc.uji.es.

to powder in order to lower the sintering temperature and accelerate the densification process (Ref 24, 25).

All coatings were sprayed on austenitic stainless steel coupons of dimensions 150 × 30 × 2 mm^3.

2.2 Feeding-Powder Characterization Techniques

Both powders were completely characterized before deposition. First, the crystalline phases were determined using X-ray diffraction (XRD) techniques (Bruker D8). Then the powders were observed by scanning electron microscopy (SEM) using a Jeol 6300 equipment. In the case of the nanostructured powder, a sample was prepared for transmission electron microscopy (TEM, Philips CM10) and the average particle size was determined from 10 TEM micrographs.

2.3 Coatings Processing

The coatings were obtained by APS using a Sulzer-Metco F4 MB plasma gun, moved by an industrial robot. Before spraying, the substrate was grit-blasted with corundum at a pressure of 3.2 bar and cleaned using ethanol in order to remove remaining dust or grease from the surface. During the process, the material to be deposited is injected in powder form using argon as carrier gas.

The use of a bond coat and a careful control of the substrate temperature during all the process were necessary to optimize the adhesion. The main spraying parameters are listed in Table 2.

2.4 Coatings Characterization Techniques

Coatings crystalline phases were evaluated by XRD analysis (Bruker D8). The coating microstructures were investigated by SEM and TEM. For each type of coated samples, two different cross sections (about 15 × 2 mm^2) were observed by SEM using a FEI Quanta 200F Field Emission Gun-SEM, connected to an X-ray energy dispersion (EDX) microanalysis equipment. The microstructure characterization was completed by TEM studies, using a Philips CM20 TEM. Thin foils for TEM observations were prepared using a focused ion beam system (FEI Dual Beam with Omniprobe pick up system).

Different coating properties were also studied. Vickers microhardness values were determined by realizing 10 indentations with a charge of 200 g for 15 s using a LECO M400 microhardness tester. The tribological behavior was characterized using a pin-on-disc tribometer (MT2/60/SCM/T from Microtest). The tests were conducted at a constant sliding speed (0.1 m/s) with a 100 m distance and a force of 5 N. The ball used was made of alumina with a hardness of 2400 HV. Microhardness measurements and wear resistance characterization were made on polished surfaces.

Table 1 Al_2O_3-TiO_2 commercial powders characteristics (supplier information)

	Conventional powder	Nanostructured powder
Supplier	Sulzer Metco, Hattersheim, Germany	Inframat Advanced Materials, Willington, USA
Product reference	METCO 130	Nanox™ S2613S
Al_2O_3:TiO_2 weight ratio	87:13	87:13
Additives	…	CeO;ZrO_2
Particles size	15-53 μm	50-500 nm
Agglomerate size	…	30 μm

3. Results and Discussion

3.1 Feeding Powders Characterization

The powders crystalline structure was determined using XRD analysis (Fig. 1). In both cases, aluminum oxide was found as corundum (α-Al_2O_3), whereas titanium oxide was mainly composed of anatase with a low proportion of rutile. In the case of the micrometric powder, traces of other titanium oxides (Ti_2O_3 and Ti_5O_9) were also identified. Concerning the reconstituted nanostructured powder, XRD analysis confirmed the presence of the additives (CeO_2 in cerianite form and ZrO_2 as zirconia and baddeleyite). SEM observation revealed that the conventional powder is formed by angular particles between 20 and 60 μm while nanostructured powders contained highly

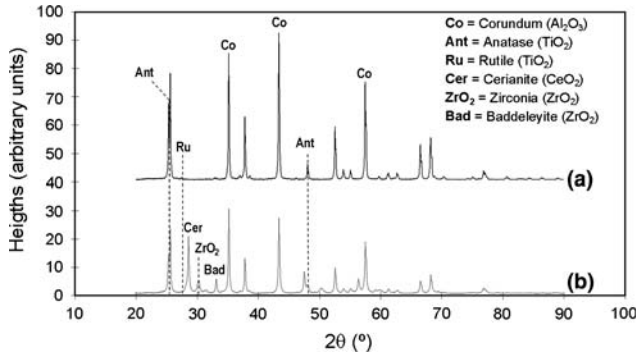

Fig. 1 XRD patterns of (a) conventional and (b) nanostructured Al_2O_3-13wt.% TiO_2 thermal spray powders

Table 2 Spraying parameters

Material	Ar, slpm	H_2, slpm	Intensity, A	Spraying distance, mm	Spraying velocity, mm/min	Mass rate, g/min
Ni-Al (bond coating)	45	11	600	140	1000	80
Al_2O_3-TiO_2						
Standard	35	12	600	120	1000	45
Variation	…	…	500-700	100-140	250-1000	…

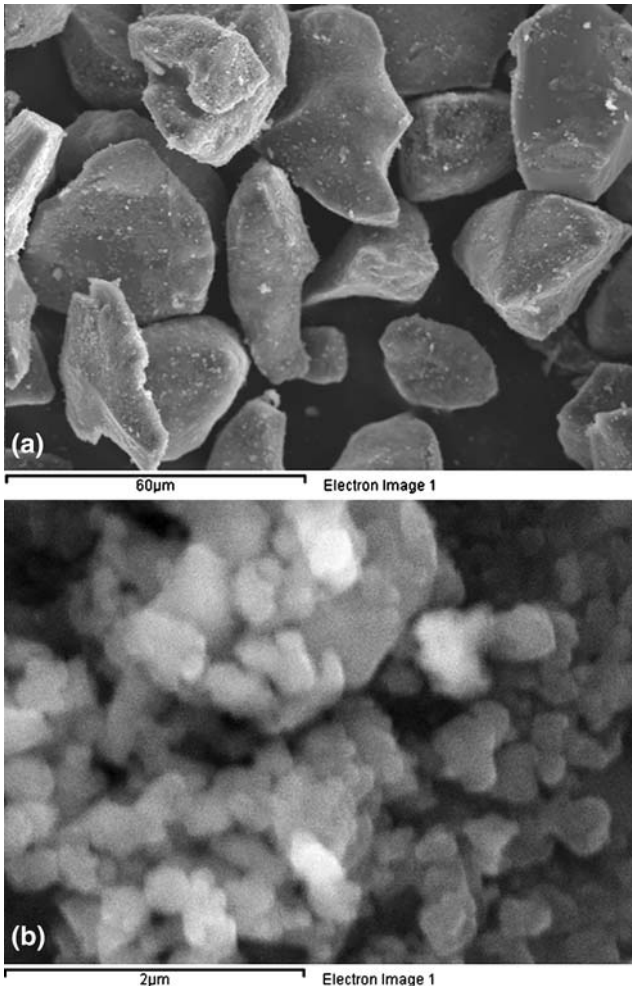

Fig. 2 SEM micrographs of (a) conventional and (b) nanostructured Al_2O_3-13wt.% TiO_2 thermal spray powders (secondary electron mode)

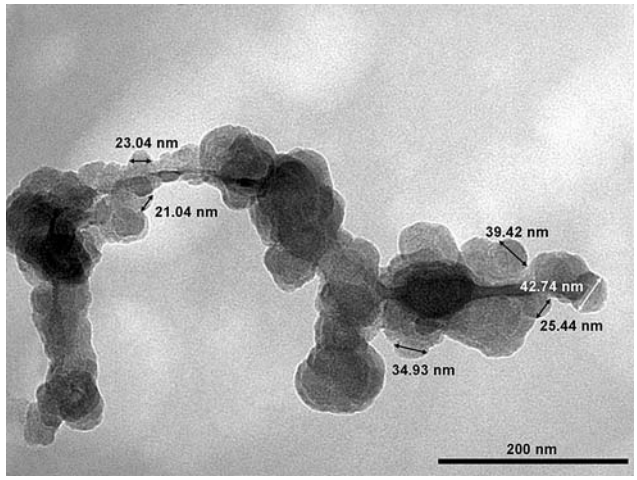

Fig. 3 TEM micrograph of the nanostructured Al_2O_3-13wt.% TiO_2 thermal spray powder

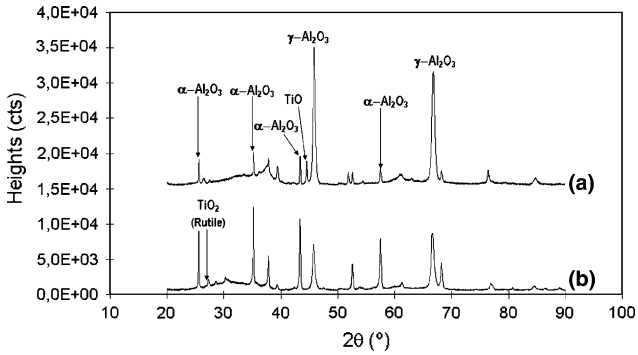

Fig. 4 XRD patterns of Al_2O_3-TiO_2 plasma-sprayed coatings (standard spraying parameters, see Table 2) using (a) conventional or (b) nanostructured powders

porous agglomerates of small particles (Fig. 2). In the nanostructured case, EDX analysis indicates that some CeO_2 is segregated, whereas the other oxides seem to be quite intimately mixed.

As an example, a TEM micrograph of the nanopowder is given in Fig. 3, with an indication of the size of some nanoparticles. The average particle size was found to be 28 ± 8 nm, which confirm the nanostructure nature of the feedstock (the mean particle size measured is even smaller than the supplier data).

3.2 Coatings Characterization

3.2.1 Microstructural Analysis. The general crystalline composition of the ceramic coatings was analyzed by XRD. The main crystalline phases found are α-Al_2O_3 (corundum), γ-Al_2O_3, and TiO_2 (rutile and brookite).

In general, the nanostructured coatings presented a higher ratio of α- to γ-alumina than their conventional counterparts, as Fig. 4 indicates. Changing the spraying parameters does not modify the crystalline phases in the coatings, although their relative proportion may vary. In fact it was observed that a lower spraying velocity allowed the deposition of coatings with a higher corundum content, especially in the case of conventional coatings, as reported elsewhere (Ref 26). This result can be explained considering that during the deposition process the powder is fused in the plasma flame and γ-alumina is formed. As the particles in the coatings cool more slowly at lower spraying velocities, more γ-Al_2O_3 is able to transform back to corundum. However, in the case of the nanostructured coatings, a slower cooling rate might induce excessive grain growth with loss of the initial nanostructure. As a consequence, a more convenient approach for obtaining a larger quantity of corundum is using a shorter spraying distance (Ref 26). As the residence time at high temperature is shorter, part of the initial corundum does not transform to γ-alumina, and remains in the final coating, preserving the initial powder nanostructure.

Coatings cross sections were observed by SEM in backscattered electron mode (BSE) sensible to the local composition. Typical micrographs can be seen in Fig. 5 and 6 for the conventional and nanostructured coatings, respectively. Figure 7 shows also a higher magnification

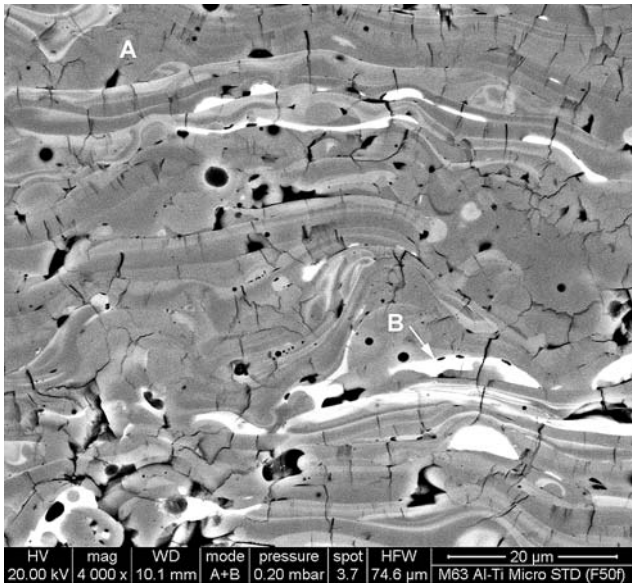

Fig. 5 Typical SEM/BSE micrograph of the Al_2O_3-TiO_2 coating obtained from the conventional powder. A, γ-alumina with a low quantity of Ti; B, titanium oxide (standard spraying parameters, see Table 2)

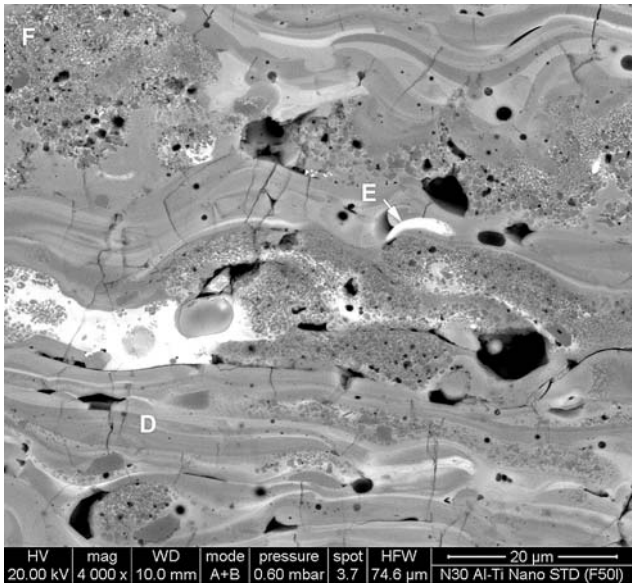

Fig. 6 Typical SEM/BSE micrograph of the Al_2O_3-TiO_2 coating obtained from the nanostructured powder. D, matrix of γ-alumina with Ti, Zr, and Ce; E, γ-alumina with Ti (may contain Zr or Ce); F, γ- and α-alumina with Ti (standard spraying parameters, see Table 2)

SEM/BSE micrograph of the coating obtained from the nanostructured powder using standard spraying parameters (Table 2) showing the presence of some agglomerate-like particles.

EDX analysis was performed to determine the atomic composition of the different phases found in the coatings. Comparing those results with those of XRD analysis, the likely phase composition of each zone in the coating

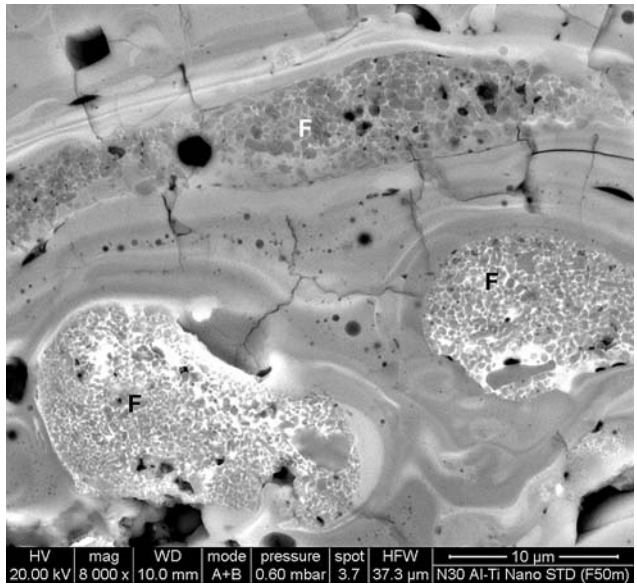

Fig. 7 SEM/BSE micrograph of the Al_2O_3-TiO_2 coating obtained from the nanostructured powder showing the agglomerate-like particles referenced as F (standard spraying parameters, see Table 2)

microstructure could be deduced. Typical results of the EDX analysis for conventional and nanostructured coatings are presented in Fig. 8 and 9, respectively.

Both nanostructured and conventional coatings are confirmed to be formed by a completely melted matrix of γ-Al_2O_3 with dissolved Ti^{+4} containing clear splat-like particles with high TiO_2 content. Few dark corundum particles were also found and, in the case of the nanostructured coatings, agglomerated-like particles (Fig. 7).

EDX analysis of the different phases shows a major difference between conventional and nanostructured coatings. As can be seen in Fig. 8(a, b) and 9(a, b), both coatings have a similar matrix composition but conventional coatings present a segregation of titanium in the white zones which show a lower aluminum content and much higher titanium proportion. In the nanostructured coating, however, the white zones have in general similar concentration of aluminum than the matrix with slightly higher titanium content. But it was also found that oxide additives may be segregated in some of the particles, as illustrated in Fig. 9(c) in the case of zirconium.

The TEM observations showed that some layers, in both types of plasma-sprayed coatings, solidified in an amorphous state, easily recognizable by a uniform grey contrast (Fig. 10a, b). Other layers were filled with columnar crystallites growing perpendicularly to the substrate, i.e. layer height. The coatings obtained with nanostructure powders were characterized by a much finer columnar size and the crystallites showed a rougher arrangement (Fig. 11a, b).

The coatings deposited from nanostructured material differed from the conventional ones in having spherical porous areas. A more detailed investigation indicated that

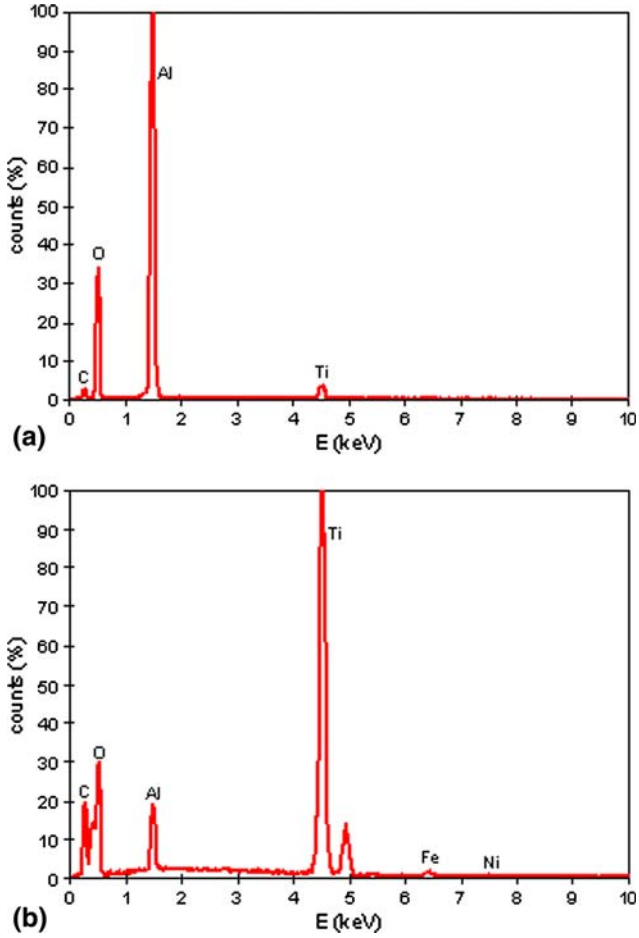

Fig. 8 Typical EDX analysis of conventional Al_2O_3-13wt.% TiO_2 coating of (a) matrix (A) and (b) white areas (B) (see SEM image in Fig. 5)

these areas are made up of an amorphous matrix of Ti, Zr, and Ce (with an unspecified amount of oxygen) surrounding globular alumina precipitates (Fig. 12 a, b).

3.2.2 Microhardness and Wear Resistance Tests. Results of the microhardness tests on conventional and nanostructured coatings obtained under different spraying conditions are shown in Table 3. Taking into account the scattering of the measurements (relative error of 5-10%), it was confirmed that nanostructured coatings have a slightly higher average microhardness value than conventional ones and that microhardness values are less affected by variations in the spraying parameters. Vickers microhardness values of conventional coatings vary between 6.4 and 8.8 GPa, whereas the nanostructured coating microhardness values are in the range 7.4-8.5 GPa.

Of the three spraying parameters studied, the spraying distance (d) has the greatest influence on the microhardness of the nanostructured coatings. The arc intensity (I) was found to have no influence on coating hardness. Although spraying distance exhibited some influence on nanostructured coating hardness, this effect was much less than in the case of the conventional coatings.

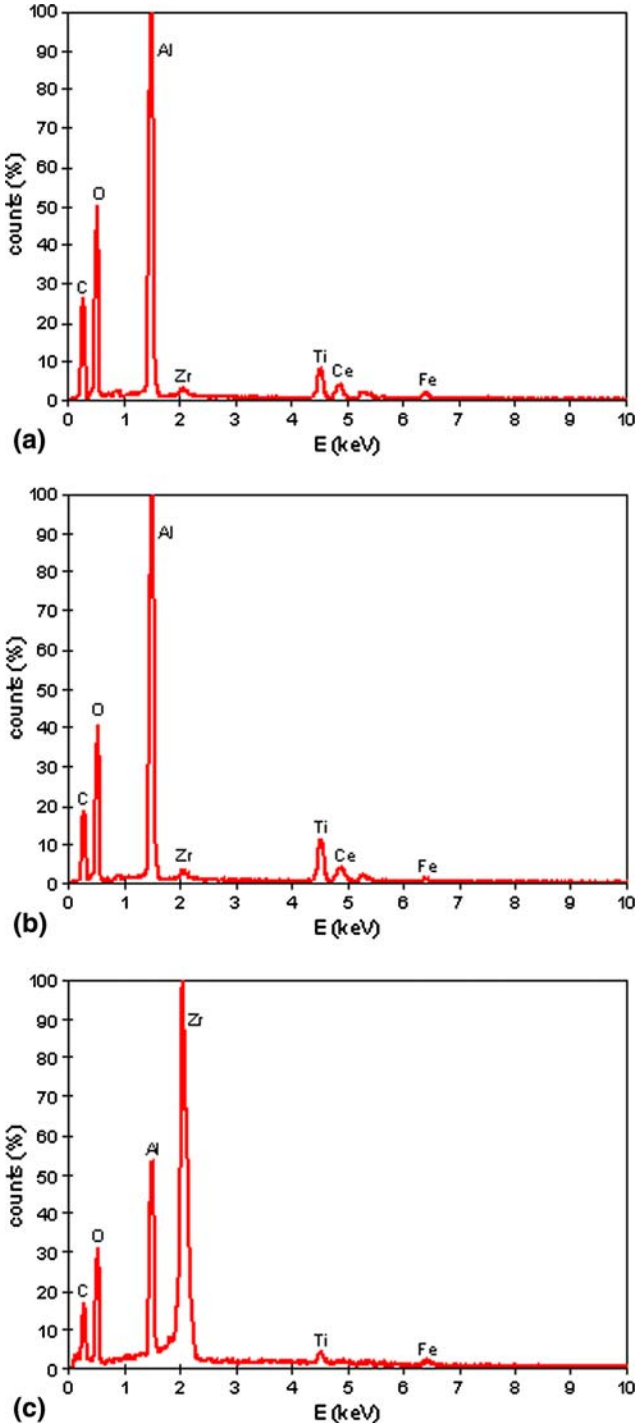

Fig. 9 Typical EDX analysis of nanostructured Al_2O_3-13wt.% TiO_2 coating of (a) matrix (C) and (b, c) two different white areas (D) (see SEM image, Fig. 6)

Regarding coating wear resistance, the tribological test conducted in this study was based on pin-on-disc experiments. According to the literature (Ref 27), in this test configuration, the predominant wear mechanism is of abrasive type and causes the material to delaminate owing to the high pressure exerted by the pin on the sample and

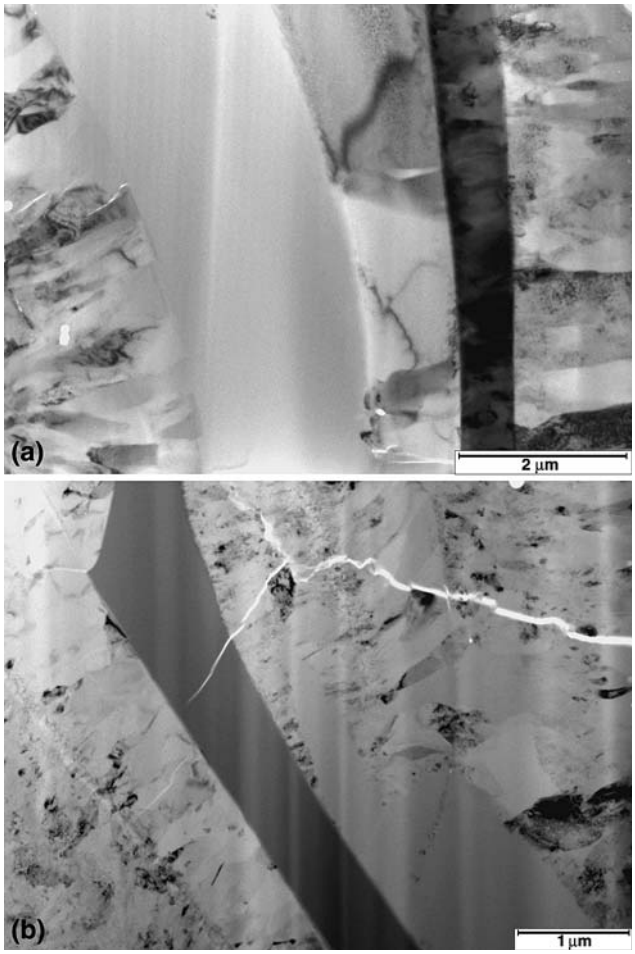

Fig. 10 TEM cross section microstructure of (a) conventional and (b) nanostructured Al_2O_3-TiO_2 coatings showing amorphous layers of uniform grey contrast inserted in-between crystalline layers

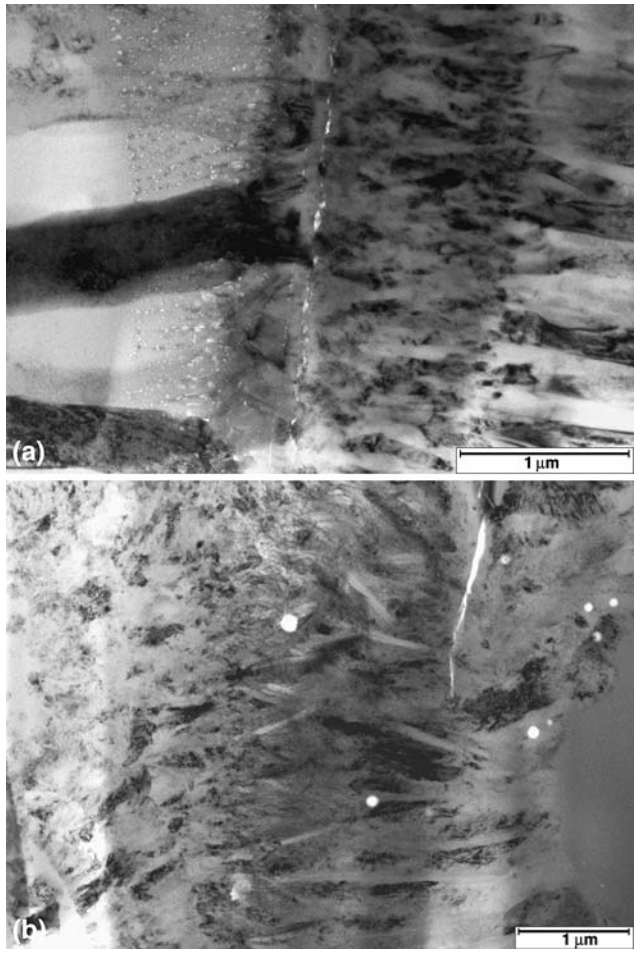

Fig. 11 TEM cross section microstructure of (a) conventional and (b) nanostructured Al_2O_3-TiO_2 coatings presenting typical shape and size of columnar crystallites

the relatively small contact area. The tribological study indicated that the nanostructured coatings had a higher wear resistance, as illustrated in Fig. 13, which shows the wear loss for the different coatings. All nanostructured coating specimens tested exhibited similar wear loss values, whereas there were differences in wear loss among the conventional sprayed coatings. The lower friction coefficient obtained for the nanostructured coatings compared with that for conventional coatings under standard conditions (0.7 and 0.9, respectively) confirmed the overall tribological behavior observed in both coatings.

The better tribological performance of the nanostructured coatings cannot be explained by their slightly higher hardness values but is probably due to the major differences observed in their microstructure in comparison to conventional coatings. First, partially fused agglomerates (marked as F in Fig. 4 and 7) were found in the nanostructured coatings and their presence can potentially impede the propagation of any crack generated in the sprayed layer since the fracture toughness of agglomerates should be higher than that of the matrix (Ref 28).

Moreover, all the titanium in the conventional samples was segregated in the white, inter-splat area (see Fig. 8 and 9). The presence of segregated titanium-rich zones at the splats boundaries leads to greater delamination and can considerably reduce the wear resistance of the conventional coatings (Ref 18). When the nanostructured feedstock is used, a uniform distribution of the titanium was observed probably due to the presence of the additives. Indeed, the role of the additives to promote solid solutions in Al_2O_3-TiO_2 mixture has recently been highlighted by Yang et al. (Ref 24). As a consequence the splat boundaries of the nanostructured coatings are less prone to delamination which explains the improvement of the wear behavior observed when the nanostructured feedstock is used.

These microstructural aspects and their influence on wear behavior were confirmed by SEM micrographs of the wear tracks produced on both coatings (Fig. 14a, b). It may be observed that the wear track on the nanostructured coating (Fig. 14b) displays a smoother or leveller appearance than that on the conventional

coating (Fig. 14a). During the test, increased delamination occurred in the micrometric coating, giving rise to large craters and cracks that propagated through the splat boundaries as a result of the stresses generated during the test, highlighting the poor adhesion between the substrate and the coating (Ref 29). It should also be pointed out that the fracture toughness of the coatings, not measured in this study, plays also a key role in determining the wear resistance of the coatings. It is the ratio of hardness to fracture toughness, called the brittleness index (B) (Ref 30), which determines the relative wear resistance of brittle materials (Ref 31, 32). In future experiments, the brittleness index of conventional and nanostructured coatings produced by different spraying conditions will be calculated and related to the wear resistance data in order to optimize the coating procedure for improved wear resistance.

In both microhardness and tribological tests, it was found that the nanostructured coatings performance is little influenced by changes in the spraying parameters, especially in the arc intensity. A possible explanation resides in the fact that METCO 130 powder is very dense, whereas Inframat S2613S powder is highly porous. As a result, the former exhibits higher thermal conductivity and is more sensitive to variations in flame temperature than the latter. This would explain the higher sensitivity of the conventional powder to spraying conditions. Moreover, the lower heat conductivity of the nanopowder would allow retention of part of the initial nanostructure, as the material does not completely fuse during the coating process. In addition, the final microstructure would also be less sensitive to the spraying conditions and, as a consequence, the wear resistance.

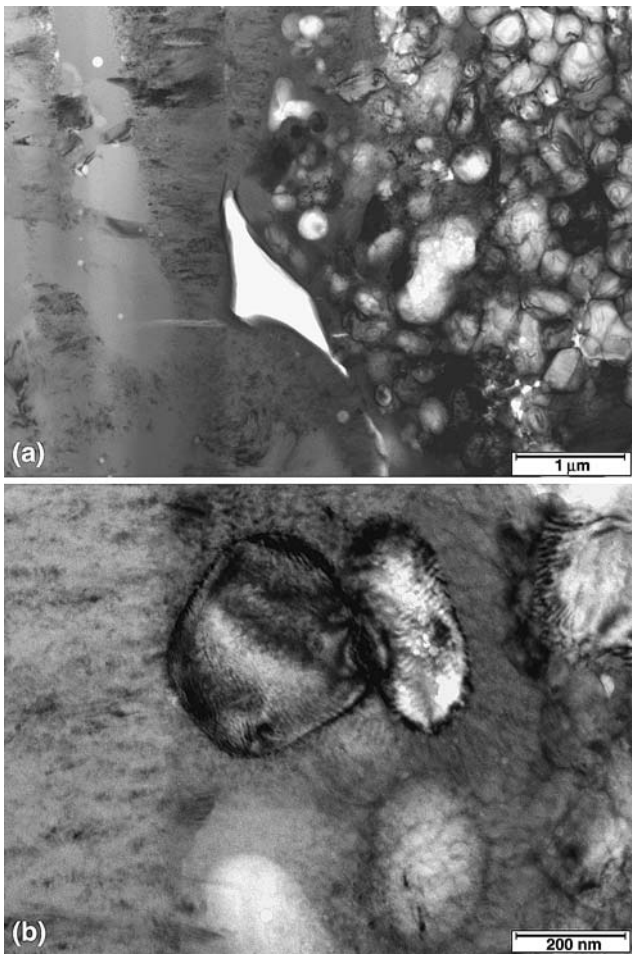

Fig. 12 TEM microstructure presenting globular alumina crystallites formed in spherical areas/inclusions found in the nanostructured Al_2O_3-TiO_2 coating (Fig. 7)

4. Conclusions

Atmospheric plasma spraying was used to Al_2O_3-13%TiO_2 coatings from conventional (micron-sized) and nanostructured powders. The microstructure comprised a completely fused region, formed mainly by nanometer-sized grains of γ-Al_2O_3 with dissolved Ti^{+4}, and a second region, which was only partly fused, retaining to a large extent the microstructure of the starting powder. As titanium segregation adversely affects wear resistance, this main microstructural difference was considered to explain

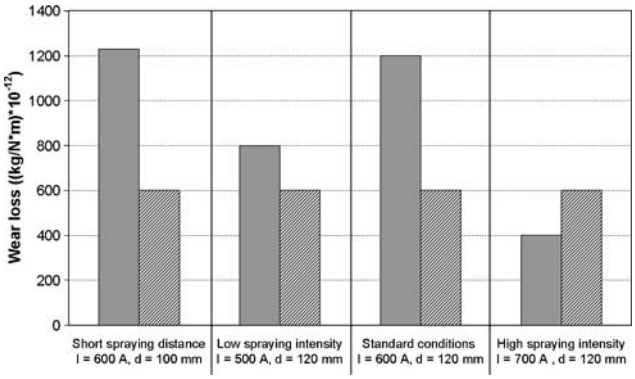

Fig. 13 Wear loss of conventional coatings (grey columns) and nanostructured coatings (striped columns) determined by pin-on-disc experiments

Table 3 Vickers microhardness of Al_2O_3-12wt.% TiO_2 coatings

Spraying parameters						
I, A	500	600	700	800	600	600
d, mm	120	120	120	120	100	140
Coating from conventional powder, GPa	7.2 ± 0.4	7.6 ± 0.3	8.8 ± 0.2	7.2 ± 0.6	7.8 ± 0.8	6.4 ± 0.9
Coating from nanostructured powder, GPa	8.5 ± 0.3	8.4 ± 0.4	8.4 ± 0.3	7.8 ± 0.7	8.2 ± 0.3	7.4 ± 0.2

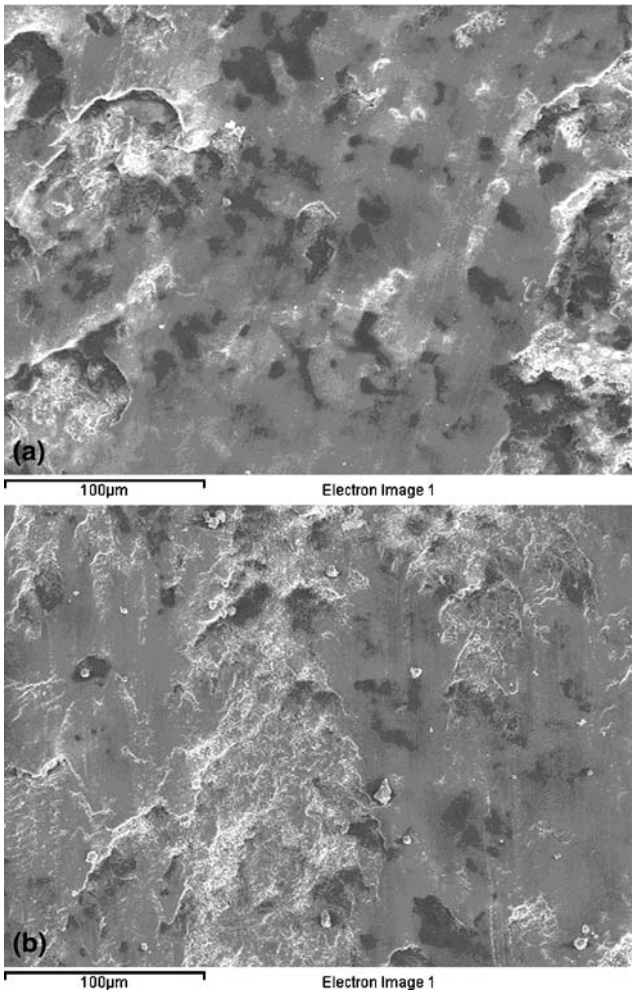

Fig. 14 Comparison of the abraded surface after the pin-on-disc test of (a) conventional coating and (b) nanostructured coating

the better tribological performance of nanostructured coatings. Moreover, the nanostructured coatings obtained exhibit greater microhardness than their conventional counterparts, and their properties are less influenced by changes in the plasma spraying parameters. Coating density, microstructural characteristics, crystallinity, grain size, and hardness were determined or inferred and it was confirmed that spraying conditions can influence these parameters differently, depending on the initial powder being conventional (micron-sized) or nanostructured.

Acknowledgments

The authors thank the EU Network of Excellence ''Knowledge-based Multicomponent Materials for Durable and Safe Performance'' (KMM-NoE, NMP3-CT-2004-502243) for financial support. They are also grateful for the support of the Valencian Institute of Small and Medium-Sized Enterprises (IMCITA/2005/2-IMCOCA/2006/1) and of the Spanish Department for Education and Sciences (MAT2006-12945-C03).

References

1. H. Gleiter, Nanostuctured Materials: Basic Concepts and Microstructure, *Acta Mater.*, 2000, **48**, p 1-29
2. E. Roduner, Size Matters: Why Nanomaterials are Different, *Chem. Soc. Rev.*, 2006, **35**, p 583-592
3. R.W. Siegel, Nanostructured Materials: Mind over Matter, *Nanostruct. Mater.*, 1993, **3**(1-6), p 1-18
4. K. Jia and T.E. Fischer, Abrasion Resistance of Nanostructured and Conventional Cemented Carbides, *Wear*, 1996, **200**, p 206-214
5. S.C. Tjong and H. Chen, Nanocrystalline Materials and Coatings, *Mater. Sci. Eng. R*, 2004, **45** (1-2), p 1-88
6. M. Gell, Application Opportunities for Nanostructured Materials and Coatings, *Mater. Sci. Eng. A*, 1995, **204**, p 246-251
7. N.B. Dahotre and S. Nayak, Nanocoatings for Engine Application, *Surf. Coat. Technol.*, 2005, **194**, p 58-67
8. S.C. Tung and M.L. McMillan, Automotive Tribology Review of Current Advances and Challenges for the Future, *Tribol. Int.*, 2004, **37**, p 517-536
9. R.B. Heimann, Applications of Plasma-Sprayed Ceramic Coatings, *Key Eng. Mater.*, 1996, **122-124**, p 399-442
10. P. Fogarassy, D. Gerday, and A. Lodini, Agglomerated Nanostructured Particles Disintegration during the Plasma Thermal Spraying Process, *Mech. Res. Commun.*, 2005, **32**, p 221-239
11. J.-H. Kim, H.-S. Yang, K.-H. Baik, B.G. Seong, C.-H. Lee, and S.Y. Hwang, Development and Properties of Nanostructured Thermal Spray Coatings, *Curr. Appl. Phys.*, 2006, **6**, p 1002-1006
12. J. He and J.M. Schoenung, A Review on Nanostructured WC-Co Coatings, *Surf. Coat. Technol.*, 2002, **157**, p 72-79
13. E.P. Song, J. Ahn, S. Lee, and N.J. Kim, Microstructure and Wear Resistance of Nanostructured Al_2O_3-8wt.% TiO_2 Coatings Plasma-Sprayed with Nanopowders, *Surf. Coat. Technol.*, 2006, **201**, p 1309-1315
14. L.L. Shaw, D. Goberman, R. Ren, M. Gell, S. Jiang, Y. Wang, D.T. Xiao, and P.R. Strutt, The Dependency of Microstructure and Properties of Nanostructured Coatings on Plasma Spray Conditions, *Surf. Coat. Technol.*, 2000, **130**, p 1-8
15. J. He and J.M. Schoenung, Nanostructured Coatings, *Mater. Sci. Eng. A*, 2002, **336**, p 274-319
16. E.H. Jordan, M. Gell, Y.H. Sohn, D. Goberman, L. Shaw, S. Jiang, M. Wang, T.D. Xiao, Y. Wang, and P. Strutt, Development and Implementation of Plasma Sprayed Nanostructured Ceramic Coatings, *Surf. Coat. Technol.*, 2001, **146-147**, p 48-54
17. Y. Zeng, S.W. Lee, and C.X. Ding, Plasma Spray in Different Nanosize Alumina, *Mater. Lett.*, 2002, **57**, p 495-501
18. J. Ahn, B. Hwan, E.P. Son, S. Lee, and N.J. Kim, Correlation of Microstructure and Wear Resistance of Al_2O_3-TiO_2 Coatings Plasma Sprayed with Nanopowders, *Metall. Mater. Trans. A*, 2006, **37**, p 1851-1861
19. X. Lin, Y. Zeng, S.W. Lee, and C. Ding, Characterization of Alumina-3 wt% Titania Coating Prepared by Plasma Spraying of Nanostructured Powders, *J. Eur. Ceram. Soc.*, 2004, **24**, p 627-634
20. Y.C. Zhu, K. Yukimura, C.X. Ding, and P.Y. Zhang, Tribological Properties of Nanostructured and Conventional WC-Co Coatings Deposited by Plasma Spraying, *Thin Solid Films*, 2002, **388**(1-2), p 277-282
21. X.Q. Zhao, H.D. Zhou, and J.M. Chen, Comparative Study of the Friction and Wear Behavior of Plasma Sprayed Conventional and Nanostructured WC-12%Co Coatings on Stainless Steel, *Mater. Sci. Eng. A*, 2006, **431**, p 290-297
22. H. Chen and C.X. Ding, Nanostuctured Zirconia Coating Prepared by Atmospheric Plasma Spraying, *Surf. Coat. Technol.*, 2002, **150**, p 31-36
23. R.S. Lima, A. Kucuk, and C.C. Berndt, Integrity of Nanostructured Partially Stabilized Zirconia after Plasma Spray Processing, *Mater. Sci. Eng. A*, 2001, **313**, p 75-82
24. Y. Yang, Y. Wang, Z. Wang, G. Liu, and W. Tian, Preparation and Sintering Behaviour of Nanostructured Alumina/Titania Composite Powders Modified with Nano-Dopants, *Mater. Sci. Eng. A*, 2008, in press. doi:10.1016/j.msea.2008.01.068
25. A. Mimaroglu, I. Taymaz, A. Ozel, and S. Arslan, Influence of the Addition of Cr_2O_3 and SiO_2 on the Tribological Performance

of Alumina Ceramics, *Surf. Coat. Technol.*, 2003, **169-170**, p 405-407
26. E. Sánchez, V. Cantavella, E. Bannier, A. Moreno, M.D. Salvador, J. Morgiel, and J. Grzonka, Deposition and Characterisation of Nanostructured Al_2O_3-TiO_2 Coatings Obtained by Atmospheric Plasma Spraying, *Proceedings of the 10th International Conference and Exhibition of the European Ceramic Society*, J.G. Heinrich and C. Aneziris, Ed., June 17-21, 2007 (Berlin), Göller Verlag, Baden-Baden, 2007, p 1471-1477. ISBN: 3-87264-022-4
27. Y. Wang, S. Jiang, M.D. Wang, S.H. Wang, and T.D. Xiao, Abrasive Wear Characteristics of Plasma Sprayed Nanostructured Alumina/Titania Coatings, *Wear*, 2000, **237**, p 176-185
28. P. Bansal, N.P. Padture, and A. Vasiliev, Improved Interfacial Mechanical Properties of Al_2O_3-13wt% TiO_2 Plasma-Sprayed Coatings Derived from Nanocrystalline Powders, *Acta Mater.*, 2003, **51**, p 2959-2970
29. X.H. Lin, Y. Zeng, C.X. Ding, and P.Y. Zhang, Effects of Temperature on Tribological Properties of Nanostructured and Conventional Al_2O_3-3 wt.% TiO_2 Coatings, *Wear*, 2004, **256**, p 1018-1025
30. B.R. Lawn and D.B. Marshall, Hardness, Toughness and Brittleness: An Indentation Analysis, *J. Am. Ceram. Soc.*, 1979, **62**, p 347-350
31. A.R. Boccaccini, Machinability and Brittleness of Glass-Ceramics, *J. Mater. Process. Technol.*, 1997, **65**, p 302-304
32. A.R. Boccaccini, The Relationship Between Wear Behaviour and Brittleness Index in Engineering Ceramics and Dispersion Reinforced Ceramic Composites, *Interceram*, 1999, **48**(3), p 176-187